Special Section: Reactive Transport Modeling

Qiulan Zhang
S. Majid Hassanizadeh*
Amir Raoof
M.Th. van Genuchten
Saskia M. Roels

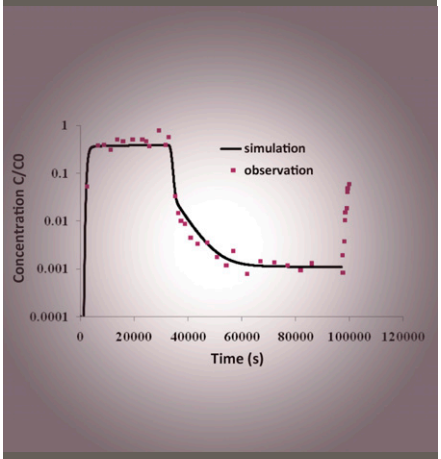

Remobilization of colloids occurs under transient flow conditions. Three different approaches were employed to simulate observed transient flow effects on the remobilization of attached viruses in sandy columns. The approach taking into account specific air-water interfacial area showed better agreement than the previously proposed models.

Q. Zhang, S.M. Hassanizadeh, and A. Raoof, Dep. of Earth Sciences, Utrecht Univ., Budapestlaan 4, 3584CD Utrecht, the Netherlands; S.M. Hassanizadeh, Soil and Groundwater Systems, Deltares, the Netherlands; M.Th. van Genuchten, Dep. of Mechanical Engineering, COPPE/LTTC, Federal Univ. of Rio de Janeiro, Rio de Janeiro, RJ 21945-970, Brazil; and S.M. Roels, Dep. of Geotechnology, Delft Univ. of Technology, Stevinweg 1, 2628 CN Delft, the Netherlands. *Corresponding author (S.M.Hassanizadeh@uu.nl).

Vadose Zone J.
doi:10.2136/vzj2011.0090
Received 20 July 2011.

Modeling Virus Transport and Remobilization during Transient Partially Saturated Flow

Virus transport in porous media is affected by the water flow regime. During transient, variably saturated flow, fluctuating flow regimes can enhance virus detachment from both solid–water interfaces (SWIs) and air–water interfaces (AWIs). The objective of this study was to simulate the influence of drainage and imbibition events on the remobilization of attached viruses. Three different modeling approaches were examined. In the first approach, all attachment and detachment coefficients were assumed to be constant, but the values of the detachment coefficients were increased drastically for the duration of transient, unsaturated flow. The second and third modeling approaches involved extensions of the model of Cheng and Saiers, who assumed enhanced detachment of viruses to be proportional to the time rate of change in the water content. Their model was extended to include separate terms for virus attachment–detachment on SWIs and AWIs. In our second approach, we assumed kinetic sorption onto the AWI, with the desorption rate being described as a function of temporal changes in the air content. This approach did not explicitly account for the specific air–water interfacial area. Thus, in our third approach we explicitly included the presence and variation of air–water interfaces and assumed AWI attachment–detachment to be an equilibrium sorption process. The available air–water interfacial area was assumed to be a function of fluid saturation. The models were used to simulate a series of saturated–unsaturated virus transport experiments reported in the literature for conditions of both drainage and imbibition. The most promising results were obtained with the third approach, which explicitly accounts for adsorption to air–water interfaces and assumes equilibrium sorption on the available air–water interfacial area.

Abbreviations: AWI, air–water interface; SWI, solid–water interface.

Studies of virus and colloid transport during transient flow in variably saturated porous media are important for devising optimal management and remediation practices for polluted water resources, especially for contaminants that may adsorb onto and migrate with colloids, including the transport of biological colloidal particles (Goyal et al., 1984; Ouyang et al., 1996). Transient-flow regimes triggered by rainfall, irrigation, snowmelt, or water table fluctuations predominate in the shallow vadose zone. Much evidence exists that fluctuating flows may remobilize deposited pathogenic microorganisms and can lead to very high peak concentrations in drinking water resources (DeNovio et al., 2004; Zhuang et al., 2007). The presence of such peak events can be a major threat to public health.

Fate and transport processes of viruses and colloids in porous media are governed by advection, dispersion, and inactivation, as well as by interactions with various interfaces (Keswick and Gerba, 1980; Yates et al., 1987; Schijven and Hassanizadeh, 2000). In unsaturated soils, the main removal processes are inactivation and attachment to solid surfaces and air–water interfaces (Powelson et al., 1990; Schijven and Hassanizadeh, 2000; Chu et al., 2001; Crist et al., 2005). These processes very much depend on prevailing hydraulic and chemical conditions that are prone to spatial and temporal changes (e.g., see Sadeghi et al. [2011] for the effect of pH and ionic strength on virus removal). Of importance to virus and colloid transport in the unsaturated zone is also the air–water interfacial area between the wetting (water) and nonwetting (air) phases, which is a function of the degree of saturation and the capillary pressure (Hassanizadeh and Gray, 1993). Much theoretical, experimental, and modeling research has recently been undertaken to understand and quantify the relationships between air–water interfacial area, capillary pressure, and fluid saturation (e.g., Pyrak-Nolte et al., 2008; Joekar-Niasar et al., 2010b).

Several studies of virus and colloid transport during variably saturated flow have shown that attachment and release are enhanced at lower degrees of saturation (e.g., Torkzaban et al., 2006a; Chu et al., 2001); however, most of these studies were performed assuming steady-state flow with uniform degrees of saturation in time and space. Commonly, a steady-state flow regime is established first before the virus transport experiments are initiated. The results of such studies are valuable in that they show the dependence of sorption or attachment–detachment parameters on fluid saturation; however, natural systems usually involve transient-flow conditions, which have been shown to often cause mobilization of attached viruses and colloids.

Gómez-Suárez et al. (1999a, 1999b, 2001b) studied the detachment of microsized particles from solid surfaces by passing air bubbles through a parallel-plate flow chamber. They varied fluid properties and hydraulic conditions to study their effects on colloid detachment. Detachment was found to decrease linearly with increasing air bubble velocity and decreasing air–water interfacial tension. The percentages of detachment by passing air bubbles also varied greatly depending on the characteristics of the bacterial strain and the solid surface (Leenaars and O'Brien, 1989; Gómez-Suárez et al., 2001a; Sharma et al., 2005; Boks et al., 2008). Results indicated that at low air bubble velocities, the hydrophobicity of the substratum had no influence on detachment. At high air bubble velocities, however, all bacterial strains were more efficiently detached from hydrophilic glass substrata. Particle shape (Gómez-Suárez et al., 2001a) and size (Gómez-Suárez et al., 2001b) were also found to be an important factor in air-bubble-induced detachment. Sharma et al. (2008a, 2008b) performed experiments similar to Gómez-Suárez et al. (1999a). They observed that an infiltrating or draining water front removed colloids that were deposited on the solid surfaces whenever the colloids came into contact with the moving AWI.

Several pore-scale visualization studies on the role of moving AWIs on colloid transport have been performed. For example, Sirivithayapakorn and Keller (2003) conducted pore-scale imbibition experiments in an unsaturated physical micromodel. They found that colloids strongly attached to the AWI. In subsequent studies, Keller and Auset (2007) showed how imbibition events thickened the water films where colloids were originally trapped and mobilized colloids attached to the AWI. They found that resaturation eventually remobilized all colloids attached to the AWI or trapped within thin water films. Crist et al. (2004, 2005) performed three-dimensional micromodel visualization experiments using a packed-sand infiltration chamber. They found that colloids not only attached to the AWI but also were trapped in thin regions where the AWI and the solid surface meet, often referred to as the air–water–solid contact line. Other pore-scale experiments on colloid transport, including retention and mobilization in unsaturated media during imbibition, were performed by Gao et al. (2006). As the water content increased and immobile water was converted to mobile water, particles were found to be released from the immobile water zones.

Several drainage and imbibition column experiments have been performed to study the remobilization of colloids and viruses as a result of transient, unsaturated flow. Results showed that the concentration of viruses at the outlet increased when a wetting front arrived (Ryan et al., 1998; Powelson and Mills, 2001; Saiers and Lenhart, 2003; Torkzaban et al., 2006a, 2006b; Shang et al., 2008; Zhuang et al., 2009; Cheng and Saiers, 2009). These studies suggest that temporal changes in saturation, whether drainage or imbibition, promote the remobilization of attached viruses and colloids.

To account for colloid remobilization during transient flow, Cheng and Saiers (2009) proposed a semi-empirical model in which the detachment coefficient is assumed to be a function of the temporal change in fluid saturation. They used the model to simulate the results of their colloid remobilization experiments. Unfortunately, the model has two shortcomings: (i) the dependency of the attachment and detachment coefficients on fluid saturation was not taken into account, and (ii) attachment to and detachment from AWIs was not specifically included in the model.

The objective of this study was to investigate the utility of the Cheng and Saiers model, and several modifications and extensions thereof, to describe experimental data reported by Torkzaban et al. (2006a, 2006b). We modified the model of Cheng and Saiers (2009) in an attempt to remove the two shortcomings mentioned above.

Column Experiments

The virus transport experiments of Torkzaban et al. (2006a, 2006b) were designed to determine the effect of water content on the attachment of viruses in soil during steady-state, unsaturated flow. They focused especially on the interaction of viruses with the SWI and AWI. In their studies, they used cylindrical polyvinyl chloride columns with an internal diameter of 10 cm and length of 23 cm. Sand with a median grain size (d_{50}) of 140 μm and uniformity coefficient (d_{60}/d_{10}) of 1.6 was packed into the columns following the procedures of Robinson and Friedman (2001) to produce as homogeneous a packing as possible. Both saturated and unsaturated flow experiments at constant flow rates and constant saturations were performed. The pH and ionic strength were also varied among the experiments. Table 1 lists the relevant parameters of the experiments. The experiments were designed such that constant saturation levels and capillary pressures existed along the column and vs. time. This was done by establishing zero pressure gradients in the column such that gravity was the only driving force for water flow.

Once steady-state flow was established, a virus suspension was added to the inlet solution. Effluent samples were taken from the

Table 1. Experimental condition of the column experiments and modeling parameters (average ± standard deviations) as reported by Torkzaban et al. (2006a, 2006b).

Parameter	Exp. LpHi100	Exp. HpLi65	Imbibition–drainage
pH	7	9	6.2
Ionic strength, mmol L^{-1}	19	0.6	19
Initial saturation, %	100	65	50
Pore water velocity, cm min^{-1}	0.68	0.56	0.46
Measured dispersivity, cm	0.06	0.44	0.56
Seeding duration, pore volumes	4.2	8.0	10.4
Column length, cm	23	23	23
Porosity (θ_s), –	0.41	0.41	0.41
Saturated hydraulic conductivity, cm min^{-1}	1.13	1.13	1.13
Soil dry bulk density (ρ_b), kg cm^{-3}	1650	1650	1650
Residual water content (θ_r)	0.055	0.055	0.055
Solid–water interface (SWI) attachment coefficient (k_{att}^s), min^{-1}	8.2 (±1.7) × 10^{-3}	0.82 (±0.34) × 10^{-3}	0.2 (±0.06) × 10^{-3}
SWI detachment coefficient (k_{det}^s), min^{-1}	1.4 (±0.2) × 10^{-3}	7.0 (±1.4) × 10^{-3}	9.5 (±1.6) × 10^{-3}
Air–water interface (AWI) attachment coefficient (k_{att}^a), min^{-1}	–	8.5 (±1.4) × 10^{-3}	1.5 (±0.06) × 10^{-3}
AWI detachment coefficient (k_{det}^a), min^{-1}	–	0.0052 (±0.001) × 10^{-3}	0.0063 (±0.001) × 10^{-3}
Inactivation rate (μ_w, μ_s, and μ_a), min^{-1}	1.3 × 10^{-5}	1.3 × 10^{-5}	1.5 × 10^{-5}
Transient condition	drained	drained	resaturated, then drained

outlet of the column at regular intervals and analyzed for virus concentrations. The virus seeding was continued until almost steady-state breakthrough curves were obtained. At the end of the seeding period, the flow of clean water and measurement of the breakthrough curve continued. Some of the steady-state experiments were followed by a transient drainage or imbibition flow phase. For transient drainage, the inflow of water at the top of the columns was terminated and the columns were allowed to drain by gravity to nearly residual water saturation. The unsaturated columns in several other transient experiments were gradually resaturated to almost full saturation by flooding them from below, after which they were drained to the residual water content. Both types of transient experiments caused steep increases in the breakthrough concentrations of the viruses, as shown by typical breakthrough curves in Fig. 1 and 2. Torkzaban et al. (2006a, 2006b) used the HYDRUS-1D code (Šimůnek et al., 1998) to model the virus experimental data during steady-state flow. They did not try to simulate the transient part of their experiments.

Mathematical Formulations

Flow in Unsaturated Porous Media

Transient flow of water through the unsaturated columns was modeled using the standard Richards equation:

$$\frac{\partial \theta}{\partial t} = \frac{\partial}{\partial x}\left[K(h)\left(\frac{\partial h}{\partial x} + 1\right)\right] \quad [1]$$

where h [L] is the water pressure head, θ (dimensionless) is the volumetric water content, K [L T^{-1}] is the hydraulic conductivity, t [T] is time, and x [L] is the vertical coordinate, taken positive in the upward direction. We used the expressions of van Genuchten (1980) to describe the nonlinear relationships between θ and h and between K and h:

$$h = -\frac{1}{\alpha}\left(S_e^{-1/m} - 1\right)^{1/n} \quad [2a]$$

$$K(h) = K_s S_e^{1/2}\left[1 - \left(1 - S_e^{1/m}\right)^m\right]^2 \quad [2b]$$

$$S_e = \frac{\theta - \theta_r}{\theta_s - \theta_r} \quad [3]$$

where θ_s and θ_r (both dimensionless) are the saturated and residual water contents, respectively, S_e (dimensionless) is the effective saturation, and α [L^{-1}], n (dimensionless), and m (dimensionless) are empirical parameters, with $m = 1 - 1/n$.

Virus Transport during Transient, Unsaturated Flow

We investigated three alternative models of virus transport during transient, variably saturated flow. The general equations governing virus transport in variably saturated media, including terms accounting for sorption onto SWIs and AWIs, as stated by Torkzaban et al. (2006b), among others, are

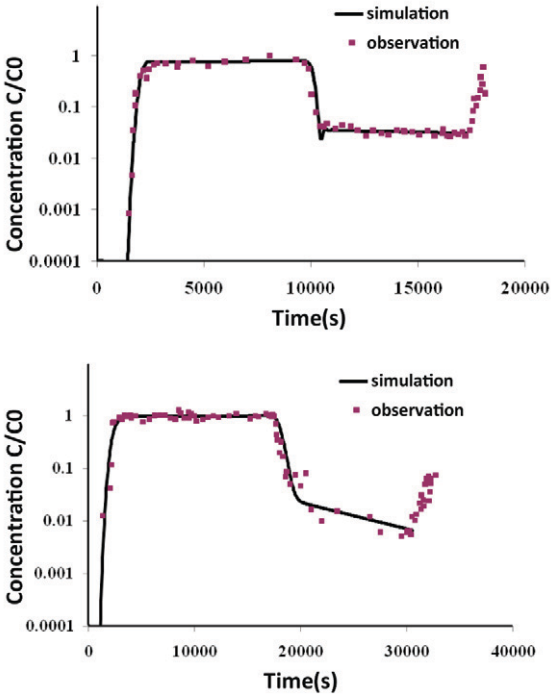

Fig. 1. Normalized virus concentration breakthrough curves at pH 7 and 100% fluid saturation (top) and pH 9 and 65% fluid saturation (bottom). Figures constructed based on data and parameter values reported by Torkzaban et al. (2006a).

$$\frac{\partial \theta C_w}{\partial t} = \frac{\partial}{\partial x}\left(\theta D \frac{\partial C_w}{\partial x}\right) - \frac{\partial q C_w}{\partial x} - \mu_w \theta C_w - \gamma_s - \gamma_a \quad [4a]$$

$$\frac{\partial \rho_b C_s}{\partial t} = \gamma_s - \mu_s \rho_b C_s = \theta k_{att}^s C_w - k_{det}^s \rho_b C_s - \mu_s \rho_b C_s \quad [4b]$$

$$\frac{\partial \theta_a C_a}{\partial t} = \gamma_a - \mu_a \theta_a C_a = \theta k_{att}^a C_w - k_{det}^a \theta_a C_a - \mu_a \theta_a C_a \quad [4c]$$

where C_w [pfu L^{-3}] is the concentration of viruses in water (number of plaque-forming units per volume of water); C_s [pfu M^{-1}] is the number of viruses adsorbed to the SWI per unit mass of dry soil; C_a [pfu L^{-3}] is the concentration of viruses adsorbed to the AWI in terms of the number of viruses per unit volume of air; ρ_b [M L^{-3}] is the soil bulk density; θ_a (dimensionless) is the air content (volume of air per unit volume of the soil); D [L^2 T^{-1}] is the dispersion coefficient, q [L T^{-1}] is the Darcy–Buckingham flow rate; γ_s and γ_a [pfu $L^{-3}T^{-1}$] are rates of adsorption to SWIs and AWIs, respectively; μ_w, μ_s, and μ_a [T^{-1}] are inactivation rate coefficients associated with the water, solid, and air phases, respectively; k_{att}^s and k_{det}^s [T^{-1}] are attachment and detachment rate coefficients, respectively, of viruses to and from the SWI; and k_{att}^a and k_{det}^a [T^{-1}] are similar attachment and detachment rate coefficients, respectively, associated with the AWI. According to Schijven and Hassanizadeh (2000), the ratio of μ_w and μ_s is generally close to unity.

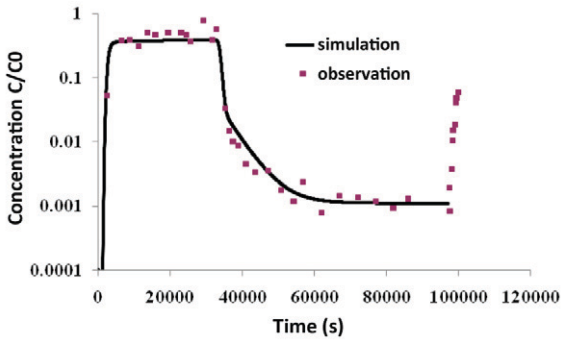

Fig. 2. Measured and fitted ϕX174 normalized virus concentration breakthrough curve for the steady-state part of the imbibition–drainage experiment (at 50% saturation) of Torkzaban et al. (2006a, 2006b).

Torkzaban et al. (2006a, 2006b) determined values of the attachment and detachment coefficients at different constant saturation values. Those data cannot be used to provide a dependence of the attachment/detachment coefficients on saturation during transient flow, however. As explained above, various researchers have reported that during both drainage and imbibition a remobilization of attached viruses may occur. One way to model this remobilization, using Eq. [4a–4c], is to assign a much larger, yet constant, value to k_{det} for the duration of a drainage or imbibition process. We shall refer to this as the *constant-detachment model*. A more physically based model was proposed by Cheng and Saiers (2009). This model was extended in two different ways to include the effect of AWIs.

Model 1: The Cheng and Saiers Model

Cheng and Saiers (2009) hypothesized that mobilization of adsorbed colloids occurs only in pores that are being emptied during drainage or are filled during imbibition. During drainage, air enters the larger pores first. As the capillary pressure increases (or water pressure decreases), smaller pores subsequently undergo drainage. The variability in pore sizes leads to a distribution of compartments (pores) that empty at a distribution of entry pressures, referred to as *snap-off pressures* by Cheng and Saiers (2009). Once a compartment empties as its entry pressure is reached, adsorbed particles are removed from the pore walls of that compartment and enter the water phase.

If the concentration of viruses that are adsorbed within the ith compartment is denoted by C_{si} (number of adsorbed viruses per unit mass of dry soil), then the total concentration adsorbed to SWIs at any given time and position is given by

$$C_s = \sum_{i=1}^{N_c} C_{si} \qquad [5]$$

where N_c is the number of compartments. Cheng and Saiers (2009) assumed that the desorption of viruses occurs as a consequence of two separate processes: a steady-state part, modeled by the standard desorption coefficient k_{det}^{s}, and an additional part accounting for mobilization of viruses from a drained compartment, modeled as $k_{det}^{i}(t)C_{si}$. Thus, under transient conditions, Eq. [4b] is extended to the following form:

$$\frac{\partial \rho_b C_s}{\partial t} = \theta k_{att}^{s} C_w - \rho_b k_{det}^{s} C_s - \rho_b \mu_s C_s - \rho_b \sum_{i=1}^{N_c} k_{det}^{i}(t) C_{si} \qquad [6]$$

where k_{det}^{i} [T^{-1}] is the transient detachment coefficient, standing for detachment from the solid grains induced by a passing AWI. This coefficient is nonzero only if the corresponding compartment is being drained. Thus, Cheng and Saiers (2009) proposed the following dependency for k_{det}^{i}:

$$k_{det}^{i} = \begin{cases} 0 & \text{for } h > h_{si} \\ N_{dr}\left|\dfrac{\partial \theta}{\partial t}\right| & \text{for } h \le h_{si} \end{cases} \qquad [7]$$

where N_{dr} (dimensionless) is an empirical coefficient that quantifies the kinetics of virus mobilization during a drainage event and h_{si} is the entry pressure head for the ith compartment. According to Eq. [7], detachment of viruses within a given compartment takes place only when the water pressure head is less than the critical water pressure head h_{si} of that compartment. Once air enters a pore, detachment occurs as long as flow is locally unsteady (i.e., $\partial\theta/\partial t \neq 0$).

The same formula is applied during imbibition, but with different restrictions because a pore fills with water when the water pressure head exceeds the critical entry (snap-off) pressure head:

$$k_{det}^{i} = \begin{cases} 0 & \text{for } h < h_{si} \\ N_{imb}\left|\dfrac{\partial \theta}{\partial t}\right| & \text{for } h \ge h_{si} \end{cases} \qquad [8]$$

where N_{imb} (dimensionless) is an empirical coefficient that quantifies the kinetics of virus mobilization during an imbibition event. The coefficients N_{dr} and N_{imb} are assumed to be the same for all compartments.

The entry pressure head distribution h_{si} for different compartments can be obtained from capillary pressure head–water content curves such as those given by Eq. [2a]. Our choice was to divide the water content range between [θ_r, θ_{ini}], where θ_{ini} is the initial water content in each transient experiment, evenly into N_c compartments, with each ith compartment then providing a corresponding value of the critical water pressure head, h_{si}. This approach assumes that viruses attach uniformly throughout the entire pore size distribution range.

Model 2: Kinetic Detachment from Air–Water Interfaces as a Function of Air Content Changes

The model of Cheng and Saiers (2009) does not specifically account for attachment to or detachment from AWIs. During imbibition, AWIs are destroyed, and viruses adsorbed onto the AWI enter the water phase. This desorption from the air phase to the water phase may be accounted for by redefining the sorption rate γ_a in Eq. [4a] and [4c] as

$$\gamma_a = \begin{cases} 0 & \text{for } h < h_{si} \\ C_a^0\left|\dfrac{\partial \theta_a}{\partial t}\right| & \text{for } h \ge h_{si} \end{cases} \qquad [9]$$

where C_a^0 is the last known concentration of AWI-adsorbed viruses before imbibition starts. Note that C_a^0 is constant in time but varies in space.

Model 3: Equilibrium Air–Water Interface Attachment–Detachment as a Function of Area

An alternative and somewhat simpler formulation may be obtained by assuming that attachment–detachment at the AWI occurs as a function of the available air–water interfacial area. The governing equation for virus transport in the liquid phase, including adsorption to SWIs and AWIs, is then obtained by adding Eq. [4a] and [4c] to eliminate γ_a, resulting in

$$\frac{\partial \theta C_w}{\partial t} + \frac{\partial a C_{aw}}{\partial t} = \frac{\partial}{\partial x}\left(\theta D \frac{\partial C_w}{\partial x}\right) - \frac{\partial q C_w}{\partial x} - \theta k_{att}^{s} C_w + \rho_b k_{det}^{s} C_s - \mu_w \theta C_w - \mu_a a C_{aw} \qquad [10]$$

where C_{aw} [pfu L^{-2}] is the concentration of viruses adsorbed to the AWI in terms of number of viruses per unit air–water interfacial area and a [L^2 L^{-3}] is the air–water interfacial area per unit volume of porous medium. This equation should be solved in conjunction with Eq. [6] for sorption onto the solid phase. Next we assume linear equilibrium partitioning of viruses between the water and air–water interface:

$$C_{aw} = K_D^a C_w \qquad [11]$$

where K_D^a [L] is the equilibrium distribution coefficient for sorption onto the AWI, expressed as $K_D^a = \theta k_{att}^a / a k_{det}^a$. Equation [10] then reduces to

$$\frac{\partial \theta R C_w}{\partial t} = \frac{\partial}{\partial x}\left(\theta D \frac{\partial C_w}{\partial x}\right) - \frac{\partial q C_w}{\partial x} - \theta k_{att}^{s} C_w + \rho_b k_{det}^{s} C_s - \mu_t \theta C_w \quad [12]$$

where

$$R = 1 + \frac{a K_D^a}{\theta} \quad [13a]$$

$$\mu_t = \mu_w + \frac{\mu_a a K_D^a}{\theta} \quad [13b]$$

Equation [12], in conjunction with Eq. [6], is applicable to both transient and steady-state saturated and unsaturated flow.

The specific air–water interfacial area (a) in the above equations is very much a transient parameter. Its value may depend not only on saturation but also on capillary pressure (Hassanizadeh and Gray, 1993; Marle, 1981; Joekar-Niasar et al., 2010a). For the purpose of this study, we assumed that a depends on water saturation, being zero when the medium is fully saturated or completely dry. We considered several specific relationships between the interfacial area, a, and the degree of fluid saturation, $S_w = \theta/\theta_s$. The best results were obtained using the following equation:

$$a = a_0 (1 - S_w)^3 S_w \quad [14]$$

where a_0 [L^2 L^{-3}] is the specific interfacial area corresponding to residual saturation of the medium. Equation [14] assumes that the effective air–water interfacial area for virus sorption increases when saturation of the medium decreases, except at very low fluid saturations when the liquid water films around particles may become too thin to allow unrestricted movement of viruses in the liquid phase to and from AWIs. The latter effect is accounted for by multiplication with S_w in Eq. [14]. This equation, without the last term (S_w), is consistent with both theoretical (e.g., Bradford and Leij, 1997; Oostrom et al., 2001) and experimental (e.g., Kim et al., 1999) analyses of air–water interfacial areas as a function of fluid saturation. The data of Kim et al. (1999) for a coarse-textured sand, similar to the one used in this study, indicate values of approximately 3 for the exponent in Eq. [14]. The value of 400 cm^{-1} for a_0, which we used in our study, was determined by using the simple power function $a = 400(1 - S_w)^3$, which is physically realistic to match the data of Kim et al. (1999).

Results

Parameter Optimization

The three different transport models presented above were solved by means of COMSOL Multiphysics 3.5a. Model parameters were estimated by fitting calculated concentration breakthrough curves to the experimental data of Torkzaban et al. (2006a, 2006b). To do so, the sum of squared residuals between calculated and measured effluent concentrations was used as the objective (or fitness) function (Raoof and Hassanizadeh, 2010). The objective function was minimized using a genetic algorithm to allow for both constrained and unconstrained optimization problems (Houck et al., 1995). Genetic algorithms differ from more traditional search algorithms in that they work with a number of candidate solutions (a population) rather than only one solution. The algorithm begins by creating a random initial population. Then at each step, individuals are selected at random from the current population and used to produce the next generation. Over successive generations, the population "evolves" toward an optimal solution (for details of the method, see Houck et al., 1995). We used in our study the Genetic Algorithm Toolbox included in Matlab (The Mathworks).

Our main objective was to estimate values of the detachment model parameters that would fit the measurements satisfactorily. Steady-state model parameter values, such as D, k_{att}^{s}, k_{det}^{s}, k_{att}^{a}, k_{det}^{a}, μ_w, μ_s, and μ_a, obtained by fitting the virus breakthrough curves with the two-site kinetic attachment–detachment model are presented in Table 1. The parameter N_c was assigned a fixed value of 5 following a sensitivity analysis (larger values did not materially change the optimization results). The hydraulic parameters α and n had to be estimated also because no water retention data were available. For this reason, we estimated these parameters as well as N_{dr} from the virus concentrations of the drainage experiment.

The van Genuchten hydraulic parameters in Eq. [2a] and [2b] for a very coarse-textured soil, in our case a medium sand with a median grain size of 140 μm and a uniformity coefficient of 1.6, are generally between 2 and 15 for n and between 14 and 35 m^{-1} for α (e.g., Schaap et al., 2001). These values were specified as limiting values in the optimization process to ensure that the parameter values remained physically realistic. The genetic algorithm repeatedly modified a population of individual solutions. In our case, each individual solution consisted of three parameter values. We used a population size of 20 individual solutions and a repetition of 10 generations.

Optimized values of the hydraulic parameters α and n and the drainage detachment constant N_{dr} are listed in Table 2. For imbibition, we used the same value of n as for drainage but shifted the drainage curve by increasing the value of α by a factor of 2 (e.g., Luckner et al., 1989). With known unsaturated soil hydraulic parameters, only the transient imbibition detachment constant N_{imb} had to be optimized. The estimated value for N_{imb} is included in Table 2.

Simulations of the Virus Transport Experiments

Simulations of the Drainage Experiments

Figure 1 presents normalized virus concentration breakthrough curves for the column experiments conducted by Torkzaban et al. (2006a) at two different fluid saturations. The solid line is the simulated breakthrough curve obtained with Eq. [4a–4b] as fitted to

Table 2. Best-fit soil hydraulic parameter values, including retention curve parameters a and n, empirical coefficients that quantify the kinetics of virus mobilization during imbibition and drainage (N_{imb} and N_{dr}, respectively), the specific interfacial area corresponding to residual saturation (a_0), the equilibrium distribution coefficient for sorption onto the air–water interface (K_D[a]), and the sum of squared residual (SSQ) for different experiments.

	Retention curve parameters		Cheng–Saiers extended model				
Experiment	α	n	N_{imb}	N_{dr}	a_0	K_D[a]	SSQ
	m^{-1}				cm^{-1}	m	
LpHi100, drainage	14.29	12.6	–	152.5 (±8.54)†	–	–	0.0137
HpLi65, drainage	14.29	12.6	–	171.5 (±7.72)	400 (±5)	0.04 (±0.01)	0.0632
Imbibition–drainage							
Imbibition‡	28.5	12.6	0.15 (±0.008)	–	400 (±5)	0.02 (±0.01)	0.0478
Drainage	14.29	12.6	–	25.59 (±1.41)	400 (±5)	0.02 (±0.003)	

† Values are plus or minus the standard error of the fitted parameter estimate.
‡ Estimated from the drainage curve.

the steady-state flow part of the curve. Corresponding parameters for the simulation are presented in Table 1. The two plots show significant increases in the virus concentration due to drainage of the column at the end of the experiments.

As discussed above, virus remobilization can be modeled in several ways: (i) increasing the otherwise constant value of the detachment coefficient, k_{det}, by some constant factor as soon as drainage or imbibition starts; (ii) changing the value of k_{det} as a function of changes in fluid saturation or air content, or (iii) changing attachment–detachment as a function of the available air–water interfacial area. Results of the three modeling approaches are compared with the experimental virus drainage data in Fig. 3. Notice that only data for the transient-flow period (and the ensuing remobilization) are shown, starting from the time when transient flow was initiated. Parameter values for the three models are listed in Tables 1 and 2. For the constant-coefficient model, the value of k_{det} was increased from 1.38×10^{-3} to 3.9×10^{-2} min^{-1} in the case of 100% fluid saturation (Exp. LpHi100) and from 7.02×10^{-3} to 6×10^{-2} min^{-1} in the case of 65% saturation (Exp. HpLi65) as determined from the optimizations. The results are shown in the top graphs of Fig. 3. It is clear that the fits are poor; even the trends in the data are not properly simulated with this model.

Results for the variable-coefficient model of Cheng and Saiers (2009) are shown in the middle graphs of Fig. 3. This model fitted the data much better than the constant-coefficient formulation. The variations in the detachment coefficient $k_{det}{}^{i}$ with time at a position 10 cm below the column inlet are shown in Fig. 4. The maximum value occurred when the drainage front reached this position. It is evident that this maximum value will be reached at later times at positions farther down the column.

Results of the modeling approach assuming linear equilibrium virus partitioning between the water phase and the available (transient) air–water interfacial area are shown in the bottom graphs of Fig. 3. Simulations using this approach provided somewhat better fits with the data than the variable detachment model of Cheng and Saiers (2009), as reflected by lower values of the sum of squared residuals between measured and calculated virus concentrations in the optimization process. Fitted parameters using this approach are listed in Table 2. The equilibrium distribution coefficients (2–4 cm) in our study were found to be several orders of magnitude larger than values (about 0.015 cm) reported by Wan and Tokunaga (1998). We do not have a good explanation for these differences, except perhaps the different experimental protocols used in the two studies (transient imbibition–drainage experiments in our study and a steady-state bubble column method of Wan and Tokunaga, 1998). Further studies about these differences are required.

Simulations of the Imbibition–Drainage Experiment

The measured breakthrough curve, including remobilization, of the imbibition–drainage experiments of Torkzaban et al. (2006a, 2006b) is shown in Fig. 2. The solid line is again the simulated breakthrough curve using the conventional virus attachment–detachment model based on Eq. [4a–4c] fitted to the steady-state flow period. The column in this case was resaturated to nearly full saturation by raising the hanging water tube and then was drained to residual water saturation.

The transient part of this experiment was simulated with the variable-detachment model as well as the formulation based on equilibrium partitioning between the water phase and air–water interfacial area during both resaturation and drainage. Optimized values of the detachment parameters N_{imb} and N_{dr}, as well as other parameters, are listed in Table 2. Figure 5 shows the measured and fitted breakthrough curves for the two approaches. The time is again presented from the start of resaturation.

As can be seen from Fig. 5, the simulations assuming equilibrium sorption onto the air–water interfacial area agree very well with the observed data. It is encouraging to see that the simpler equilibrium sorption model works as well, or better, that the numerically

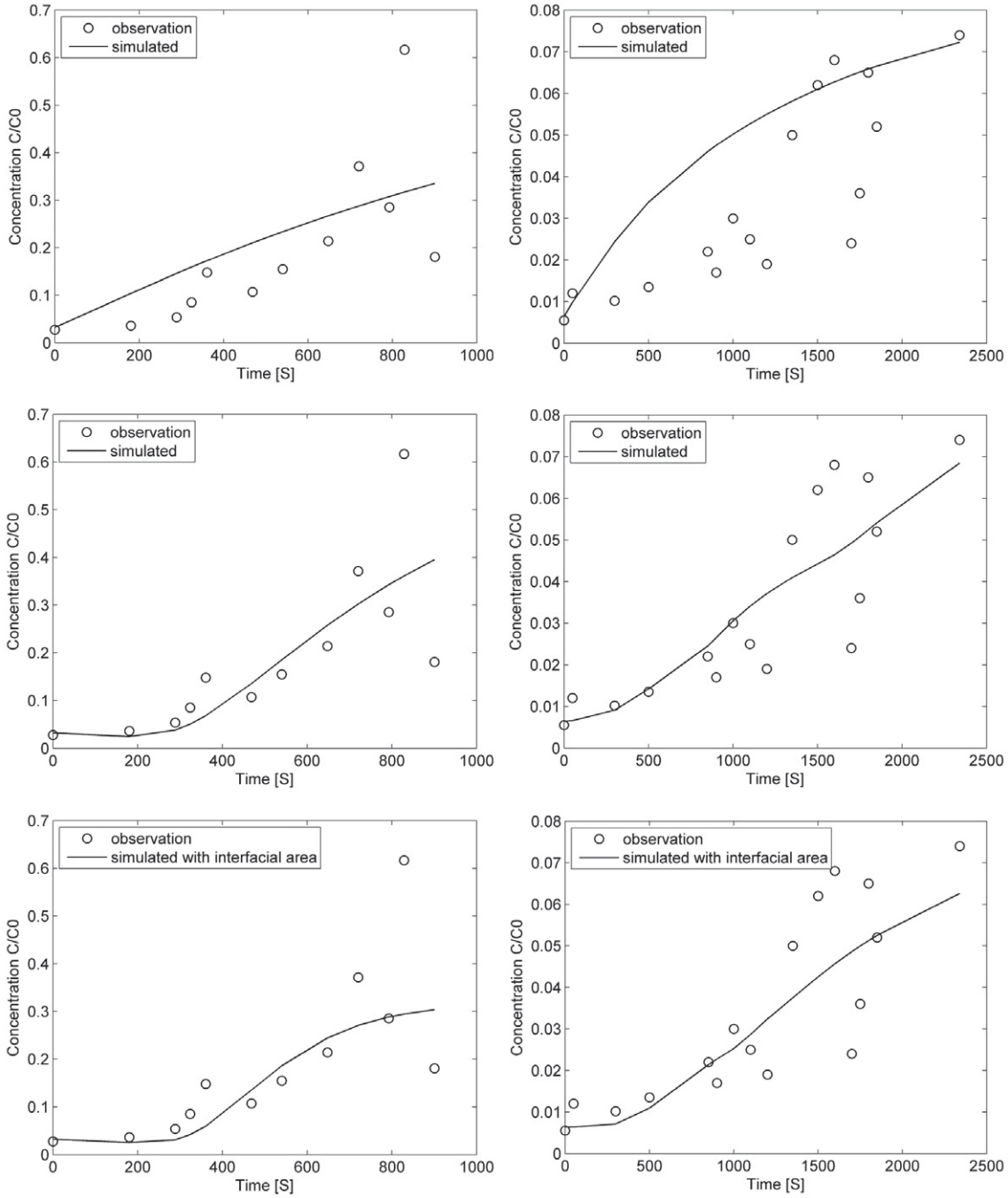

Fig. 3. Observed (open circles) and fitted (lines) virus remobilization breakthrough curves for two drainage experiments: Exp. LpHi100 (low pH, high ionic strength, 100% fluid saturation) (left) and HpLi65 (high pH, low ionic strength, 65% fluid saturation) (right) simulations assuming constant detachment rate (k_{det}) (top), variable k_{det} (middle), and equilibrium partitioning on the air–water interface (bottom).

more intricate variable detachment formulation. We note here that the formulation based on sorption onto the air–water interfacial area requires an expression relating the specific interfacial area to the degree of fluid saturation, or alternatively the air content. In this study, we used Eq. [14] for this purpose, which performed better than several other expressions we investigated for a, including simple power functions of relative fluid saturation such as $a = a_0(1 - S_w)^p$. Equation [14] suggests that, as expected, the effective AWI for virus sorption increases when the medium desaturates, except in very dry systems. Alternative expressions for Eq. [14] may need to be investigated in future work, especially for medium- and fine-textured sand.

Concluding Remarks

Virus remobilization during draining column experiments and during the processes of resaturation conducted by Torkzaban et al. (2006a, 2006b) was modeled. First, we used the constant-detachment coefficient model, which just increased the detachment coefficient by a constant factor. Then we modified the model of

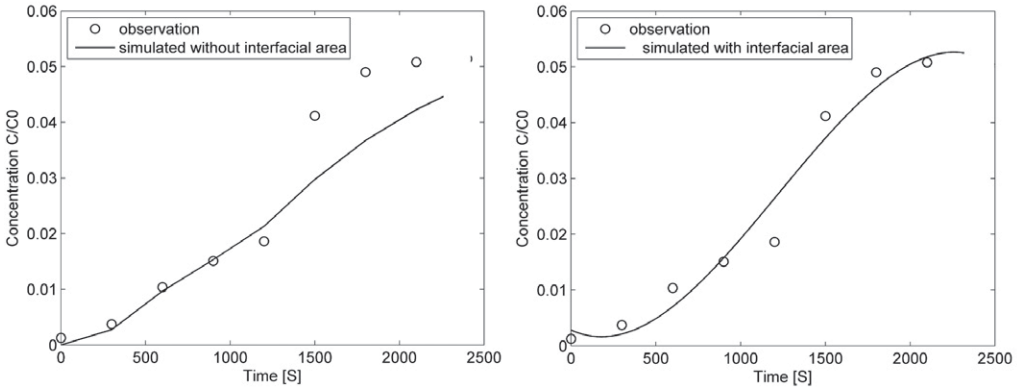

Fig. 4. Variable detachment rates (k_{det}) during drainage at 10 cm below the column inlet: drainage starting from a saturated column (left) and drainage starting from a fluid saturation of 65% (right). Vertical bars indicate the k_{det} where the compartments defined in Cheng and Saiers (2009) model are drained.

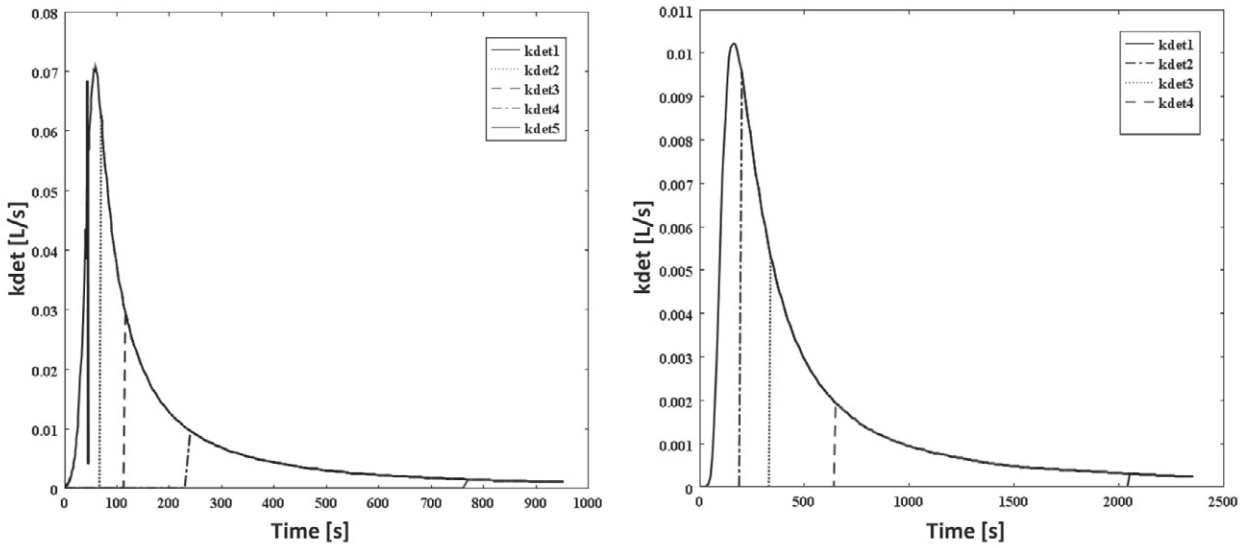

Fig. 5. Observed (open circles) and fitted (lines) virus remobilization breakthrough curves for the imbibition–drainage experiment of Torkzaban et al. (2006a, 2006b): breakthrough results using the model with air–water interface virus attachment–detachment as a function of air content (left) and as a function of the air–water interfacial area.

Cheng and Saiers (2009) by including the effect of virus attachment on AWIs. Two alternative formulations were considered; one was virus attachment–detachment on the AWI modeled as a function of transient changes in the air content, and the other was virus sorption on the AWI modeled as an apparent linear equilibrium partitioning process subject to the available (transient) air–water interfacial area (being zero at full saturation). The latter model formulation was found to fit the observed data satisfactorily. Separate SWI and AWI virus mass balances (see Fig. 6 and 7) showed that, in total, more viruses accumulated at, and released from, the SWI than the AWI.

One point needing emphasis is that the experiments of Torkzaban et al. (2006a, 2006b) showed that steady-state attachment coefficients obtained from experiments performed at different fluid saturations are different (see Table 1). This means that in drainage–imbibition experiments, the steady-state attachment coefficients $k_{att}{}^{s}$ and $k_{att}{}^{a}$ should be some function of the fluid saturation. As such, we included in our transient simulations a linear dependence of the attachment coefficient on saturation. Comparison of the results with the constant-attachment model simulations, however, showed very little difference. This may have been due to the large values of the transient detachment coefficients, which may have obscured any variations in the attachment coefficients (causing them to have little effect on the results).

We studied the effect of fluid saturation changes on colloid remobilization at the column scale. As noted by Bradford et al. (2009), among others, column scale analysis, especially if limited to breakthrough curves, provides only limited information about the exact processes involved. While important, such column-scale studies may need to be augmented with more intricate pore-scale theoretical and experimental studies to more precisely identify the underlying processes responsible for colloid remobilization during transient imbibition and drainage events. Additional research is also needed to investigate the applicability of the model of Cheng and Saiers (2009), or the formulations developed in this study, for virus transport in structured field soils as well as for two- or three-dimensional flow conditions. It is further worth noting that the recent study of Sadeghi et al. (2011) has shown that transient

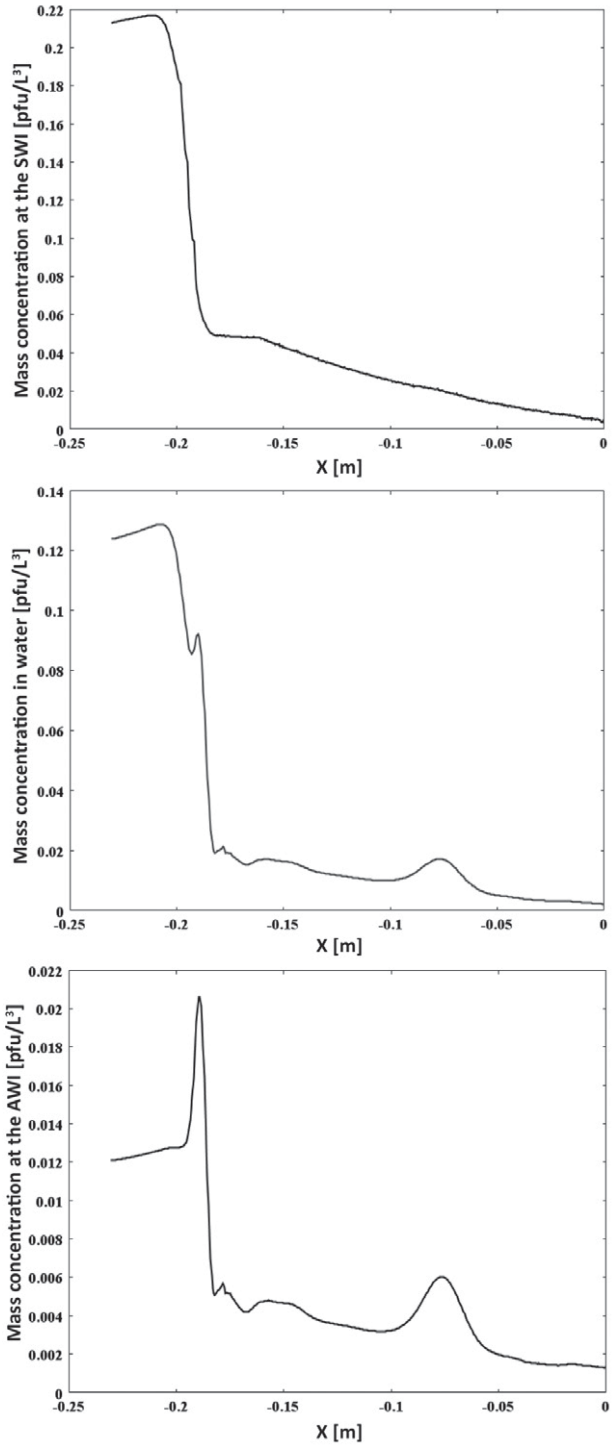

Fig. 6. Profiles of the amount of viruses being retained at the solid–water interface (SWI) ($\rho_b C_s$), in water (θC_w), and at the air–water interface (AWI) (aC_{aw}).

changes in water chemistry also result in the remobilization of adsorbed viruses. It is important to investigate which other transient effects may have similar consequences for virus transport in soil systems.

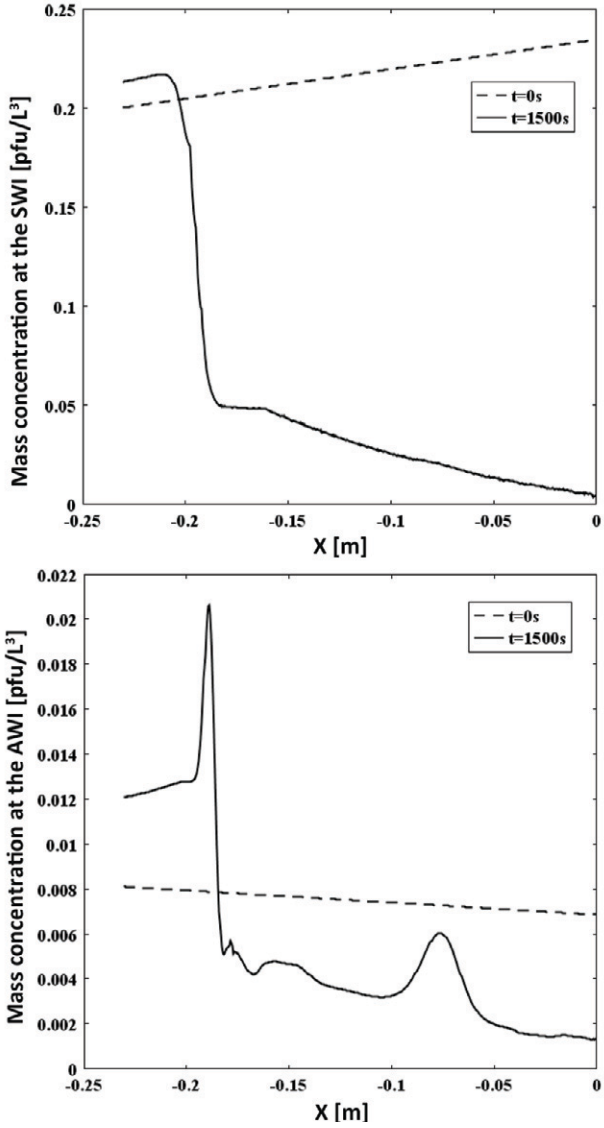

Fig. 7. Concentration profiles of viruses at the solid–water interface (SWI) and the air–water interface (AWI). Dashed lines represent concentration profiles at the very beginning of the remobilization simulation. Solid lines represent concentration profiles at the end of the remobilization simulation.

Acknowledgments

Saeed Torkzaban (CSIRO, Adelaide, Australia) is gratefully acknowledged for providing the experimental data. We are thankful to Jack Schijven (National Institute of Public Health and the Environment, the Netherlands) and Vahid Joekar-Niasar (Utrecht University, the Netherlands) for very helpful discussions. Financial help for Q. Zhang by the China Scholarship Council is greatly appreciated. We are thankful to Sabine Goldberg and three anonymous reviewers for their critical comments and valuable recommendations that helped to improve our manuscript. The first three authors are members of the International Research Training Group NUPUS, financed by the German Research Foundation (DFG) and Netherlands Organization for Scientific Research (NWO).

References

Boks, N.P., W. Norde, H.C. van der Mei, and H.J. Busscher. 2008. Forces involved in bacterial adhesion to hydrophilic and hydrophobic surfaces. Microbiology 154:3122–3133. doi:10.1099/mic.0.2008/018622-0

Bradford, S.A., and F.J. Leij. 1997. Estimating interfacial areas for multifluid soil systems. J. Contam. Hydrol. 27:83–105. doi:10.1016/S0169-7722(96)00048-4

Bradford, S.A., S. Torkzaban, F.J. Leij, J. Šimůnek, and M.Th. van Genuchten. 2009. Modeling the coupled effects of pore space geometry and velocity on colloid transport and retention. Water Resour. Res. 45:W02414. doi:10.1029/2008WR007096

Cheng, T., and J.E. Saiers. 2009. Mobilization and transport of in situ colloids during drainage and imbibition of partially saturated porous media. Water Resour. Res. 45:W08414. doi:10.1029/2008WR007494

Chu, Y., Y. Jin, M. Flury, and M.V. Yates. 2001. Mechanisms of virus removal during transport in unsaturated porous media. Water Resour. Res. 37:253–263. doi:10.1029/2000WR900308

Crist, J.T., J.F. McCarthy, Y. Zevi, P. Baveye, J.A. Throop, and T.S. Steenhuis. 2004. Pore-scale visualization of colloid transport and retention in partly saturated porous media. Vadose Zone J. 3:444–450.

Crist, J.T., Y. Zevi, J.F. McCarthy, J.A. Troop, and T.S. Steenhuis. 2005. Transport and retention mechanisms of colloids in partially saturated porous media. Vadose Zone J. 4:184–195.

DeNovio, N.M., J.E. Saiers, and J.N. Ryan. 2004. Colloid movement in unsaturated porous media: Recent advances and future directions. Vadose Zone J. 3:338–351.

Gao, B., J.E. Saiers, and J.N. Ryan. 2006. Pore-scale mechanisms of colloid deposition and mobilization during steady and transient flow through unsaturated granular media. Water Resour. Res. 42:W01410. doi:10.1029/2005WR004233

Gómez-Suárez, C., H.J. Busscher, and H.C. van der Mei. 2001a. Analysis of bacterial detachment from substratum surfaces by the passage of air–liquid interfaces. Appl. Environ. Microbiol. 67:2531–2537. doi:10.1128/AEM.67.6.2531-2537.2001

Gómez-Suárez, C., J. Noordmans, H.C. van der Mei, and H.J. Busscher. 1999a. Detachment of colloidal particles from collector surfaces with different electrostatic charge and hydrophobicity by attachment to air bubbles in a parallel plate flow chamber. Physiol. Chem. Phys. 1:4423–4427. doi:10.1039/a905156b

Gómez-Suárez, C., J. Noordmans, H.C. van der Mei, and H.J. Busscher. 1999b. Removal of colloidal particles from quartz collector surfaces as stimulated by the passage of liquid–air interfaces. Langmuir 15:5123–5127. doi:10.1021/la981608c

Gómez-Suárez, C., H.C. van der Mei, and H.J. Busscher. 2001b. Air bubble-induced detachment of polystyrene particles with different sizes from collector surfaces in a parallel plate flow chamber. Colloids Surf. A 186:211–219. doi:10.1016/S0927-7757(00)00799-8

Goyal, S.M., B.H. Keswick, and C.P. Gerba. 1984. Viruses in groundwater beneath sewage irrigated cropland. Water Res. 18:299–302. doi:10.1016/0043-1354(84)90103-9

Hassanizadeh, S.M., and W.G. Gray. 1993. Thermodynamic basis of capillary pressure in porous media, Water Resour. Res. 29:3389–3405. doi:10.1029/93WR01495

Houck, C.R., J.A. Joines, and M.G. Kay. 1995. A genetic algorithm for function optimization: A Matlab implementation. Tech. Rep. NCSU-IE-TR-95–09. North Carolina State Univ., Raleigh.

Joekar-Niasar, V., S.M. Hassanizadeh, and H.K. Dahle. 2010a. Non-equilibrium effects in capillarity and interfacial area in two-phase flow: Dynamic pore-network modelling. J. Fluid Mech. 655:38–71. doi:10.1017/S0022112010000704

Joekar-Niasar, V., M. Prodanovic, D. Wildenschild, and S.M. Hassanizadeh. 2010b. Network model investigation of interfacial area, capillary pressure and saturation relationships in granular porous media. Water Resour. Res. 46:W06526. doi:10.1029/2009WR008585

Keller, A.A., and M. Auset. 2007. A review of visualization techniques of biocolloid transport processes at the pore scale under saturated and unsaturated conditions. Adv. Water Resour. 30:1392–1407. doi:10.1016/j.advwatres.2006.05.013

Keswick, B.H., and C.P. Gerba. 1980. Viruses in groundwater. Environ. Sci. Technol. 14:1290–1297. doi:10.1021/es60171a602

Kim, H., P.S.C. Rao, and M.D. Annable. 1999. Gaseous tracer technique for estimating air–water interfacial areas and interface mobility. Soil Sci. Soc. Am. J. 63:1554–1560. doi:10.2136/sssaj1999.6361554x

Leenaars, A.F.M., and S.B.G. O'Brien. 1989. Particle removal from silicon substrates using surface-tension forces. Philips J. Res. 44:183–209.

Luckner, L., M.Th. van Genuchten, and D.R. Nielsen. 1989. A consistent set of parametric models for the two-phase flow of immiscible fluids in the subsurface. Water Resour. Res. 25:2187–2193. doi:10.1029/WR025i010p02187

Marle, C.M. 1981. From the pore scale to the macroscopic scale: Equations governing multiphase fluid flow through porous media. In: A. Verruijt and F.B.J. Barends, editors, Flow and Transport in Porous Media: Proceedings of Euromech 143, Delft, the Netherlands. 2–4 Sept. 1981. A.A. Balkema, Rotterdam, the Netherlands. p. 57–61.

Oostrom, M., M.D. White, and M.L. Brusseau. 2001. Theoretical estimation of free and entrapped nonwetting–wetting fluid interfacial areas in porous media. Adv. Water Resour. 24:887–898. doi:10.1016/S0309-1708(01)00017-3

Ouyang, Y., D. Shinde, R.S. Mansell, and W. Harris. 1996. Colloid enhanced transport of chemicals in subsurface environments: A review. Crit. Rev. Environ. Sci. Technol. 26:189–204. doi:10.1080/10643389609388490

Powelson, D.K., and A.L. Mills. 2001. Transport of *Escherichia* in sand columns with constant and changing water contents. J. Environ. Qual. 30:238–245. doi:10.2134/jeq2001.301238x

Powelson, D.K., J.R. Simpson, and C.P. Gerba. 1990. Virus transport and survival in saturated and unsaturated flow through soil columns. J. Environ. Qual. 19:396–401. doi:10.2134/jeq1990.00472425001900030008x

Pyrak-Nolte, L.J., D.D. Nolte, D. Chen, and N.J. Giordano. 2008. Relating capillary pressure to interfacial areas. Water Resour. Res. 44:W06408. doi:10.1029/2007WR006434

Raoof, A., and S.M. Hassanizadeh. 2010. A new method for generating pore-network models of porous media. Transp. Porous Media 81:391–407. doi:10.1007/s11242-009-9412-3

Robinson, D.A., and S.P. Friedman. 2001. The effect of particle size distribution on the effective dielectric permittivity of saturated granular media. Water Resour. Res. 37:33–40. doi:10.1029/2000WR900227

Ryan, J.N., T.H. Illangasekare, M.I. Litaor, and R. Shannon. 1998. Particle and plutonium mobilization in macroporous soil during rainfall simulations. Environ. Sci. Technol. 32:476–482. doi:10.1021/es970339u

Sadeghi, G., J.F. Schijven, T. Behrends, S.M. Hassanizadeh, J. Gerritse, and P.J. Kleingeld. 2011. Systematic study of effects of pH and ionic strength on attachment of phage PRD1. Ground Water 49:12–19. doi:10.1111/j.1745-6584.2010.00767.x

Saiers, J.E., and J.J. Lenhart. 2003. Colloid mobilization and transport within unsaturated porous media under transient-flow conditions. Water Resour. Res. 39:10–19. doi:10.1029/2002WR001370

Schaap, M.G., F.J. Leij, and M.Th. van Genuchten. 2001. ROSETTA: A computer program for estimating soil hydraulic parameters with hierarchical pedotransfer functions. J. Hydrol. 251:163–176. doi:10.1016/S0022-1694(01)00466-8

Schijven, J.F., and S.M. Hassanizadeh. 2000. Removal of viruses by soil passage: Overview of modeling, processes, and parameters. Crit. Rev. Environ. Sci. Technol. 30:49–127. doi:10.1080/10643380091184174

Shang, J., M. Flury, G. Chen, and J. Zhuang. 2008. Impact of flow rate, water content, and capillary forces on in situ colloid mobilization during infiltration in unsaturated sediments. Water Resour. Res. 44:W06411. doi:10.1029/2007WR006516

Sharma, P., H.M. Abdou, and M. Flury. 2008b. Effect of the lower boundary condition and flotation on colloid mobilization in unsaturated sandy sediments. Vadose Zone J. 7:930–940. doi:10.2136/vzj2007.0163

Sharma, P., M. Flury, and J. Zhou. 2008a. Detachment of colloids from a solid surface by a moving air–water interface. J. Colloid Interface Sci. 326:143–150. doi:10.1016/j.jcis.2008.07.030

Sharma, P.K., M.J. Gibcus, H.C. van der Mei, and H.J. Busscher. 2005. Influence of fluid shear and micro bubbles on bacterial detachment from a surface. Appl. Environ. Microbiol. 71:3668–3673. doi:10.1128/AEM.71.7.3668-3673.2005

Šimůnek, J., M. Sejna, and M.Th. van Genuchten. 1998. The HYDRUS-1D software package for simulating the one-dimensional movement of water, heat, and multiple solutes in variably-saturated media, Version 2.0. U.S. Salinity Lab., Riverside, CA.

Sirivithayapakorn, S., and A.A. Keller. 2003. Transport of colloids in unsaturated porous media: A pore-scale observation of processes during the dissolution of air–water interface. Water Resour. Res. 39(12):1346. doi:10.1029/2003WR002487

Torkzaban, S., S.M. Hassanizadeh, J.F. Schijven, A.M. de Bruin, and A.M. de Roda Husman. 2006a. Virus transport in saturated and unsaturated sand columns. Vadose Zone J. 5:877–885. doi:10.2136/vzj2005.0086

Torkzaban, S., S.M. Hassanizadeh, J.F. Schijven, and H.H.J.L. van den Berg. 2006b. Role of air–water interfaces on retention of viruses under unsaturated conditions. Water Resour. Res. 42:W12S14. doi:10.1029/2006WR004904

van Genuchten, M.Th. 1980. A closed-form equation for predicting the hydraulic conductivity of unsaturated soils. Soil Sci. Soc. Am. J. 44:892–898. doi:10.2136/sssaj1980.03615995004400050002x

Wan, J., and T.K. Tokunaga. 1998. Measuring partition coefficients of colloids at air–water interfaces. Environ. Sci. Technol. 32:3293–3298. doi:10.1021/es980228a

Yates, M.V., S.R. Yates, J. Wagner, and C.P. Gerba. 1987. Modeling virus survival and transport in the subsurface. J. Contam. Hydrol. 1:329–345. doi:10.1016/0169-7722(87)90012-X

Zhuang, J., J.F. McCarthy, J.S. Tyner, E. Perfect, and M. Flury. 2007. In situ colloid mobilization in Hanford sediments under unsaturated transient flow conditions: Effect of irrigation pattern. Environ. Sci. Technol. 41:3199–3204. doi:10.1021/es062757h

Zhuang, J., J.S. Tyner, and E. Perfect. 2009. Colloid transport and remobilization in porous media during infiltration and drainage. J. Hydrol. 377:112–119. doi:10.1016/j.jhydrol.2009.08.011